Ln(III) complexes as potential phosphors for white LEDs

Akerboom, S.

2 Substituted phenanthrolines as antennae in luminescent Eu(III) complexes

Eight novel europium(III)-based coordination compounds with 1,10-phenanthroline ligands with a chloro , methoxy-, ethoxy-, cyano-, carboxylic acid, methyl carboxylate-, ethyl carboxylate, and amino-substituent on the 2-position have been prepared in yields ranging from 43 to 89%. Additionally, one lanthanum(III) coordination compound of 2-amino-1,10-phenanthroline has been isolated. All compounds have the general formula $[Ln(L)_2(NO_3)_3]$, except for the compound with the carboxylate ligand, which has the formula $[Eu(O_2Cphen)_3]$. Of three of the Eu(III) complexes as well as the La(III) compound crystal structures have been determined, all showing similar N_4O_6 coordination spheres for the Ln(III) ion. Seven compounds exhibit bright luminescence characteristic of Eu(III) upon irradiation with near UV (nUV) radiation, indicating efficient ligand-to-metal energy transfer. The complex with 2-amino-1,10-phenanthroline is non-luminescent. The solid state photoluminescent quantum yields range from 10% to 79% and luminescence lifetimes vary from 0.43 to 1.57 ms. Analysis of the spectral intensities with the Judd-Ofelt theory shows a significant contribution of non-radiative processes that quench the luminescence of the $^5D_0$ level on Eu(III). In addition, 1-methyl-1,10-phenanthrolin-2(1H)-one has been used as a ligand for the first time, using Eu(III) as a central ion. The resulting complex exhibits moderately bright photoluminescence upon excitation with nUV radiation.

(Parts of this chapter have been published:
S. Akerboom, J.J.M.H. van den Elshout, I. Mutikainen, W.T. Fu, E. Bouwman, *Polyhedron* (2013), in press; S. Akerboom, J.J.M.H. van den Elshout, I. Mutikainen, M.A. Siegler, W.T. Fu, E. Bouwman, *Eur. J. Inorg. Chem.* (2013), in press)

2.1 Introduction

As discussed in Chapter 1, there is a need for highly efficient and stable red phosphor materials that can be efficiently excited in the nUV region. Complexes of Eu(III) ions with suitable antenna ligands are promising candidates for this purpose. A promising class of ligands comprises 1,10-phenanthrolines. Used either as a solitary sensitizer or as a neutral co-ligand to saturate the lanthanoid coordination sphere of complexes with anionic ligands, 1,10-phenanthrolines are capable of efficient sensitization of Eu(III)-centered luminescence [1-5]. The complex [Eu(1,10-phenanthroline)$_2$(NO$_3$)$_3$] is known to be highly luminescent, but efficient excitation at wavelengths above 355 nm is not possible [1, 6]. A redshift of the excitation maximum by at least 20 nm is required to allow for efficient excitation in the nUV range. To investigate the influence of substituents on 1,10-phenanthroline on the luminescence properties of complexes with Eu(III), a series of phenanthroline ligands with both electron-donating and electron-withdrawing substituents at the 2-position has been prepared. Coordination compounds with Eu(III) have been synthesized and their photophysical properties are reported. An overview of the compounds studied is given in Figure 2.1. During this study on the influence of substituents on 1,10-phenanthroline on the photoluminescent properties of the Eu(III) complexes, out of curiosity one of the synthetic intermediates, 1-methyl-1,10-phenanthrolin-2(1*H*)-one (**9**) shown in Figure 2.1, was used as a ligand for Eu(III). We were surprised by the relatively easy formation of a complex with a poor ketone-type ligand. Moreover, to the best of our knowledge, this molecule has never been used before as a ligand.

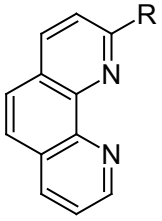

1-8

R	Ligand #	Complex #
CN	**1**	**Eu1**
COOH	**2**	**Eu2**
COOMe	**3**	**Eu3**
COOEt	**4**	**Eu4**
Cl	**5**	**Eu5**
OMe	**6**	**Eu6**
OEt	**7**	**Eu7**
NH_2	**8**	**Eu8**
		La8
	9	**Eu9**

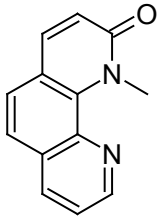

9

*Figure 2.1: An overview of the compounds described in this work. The complexes have the general formula [Ln(L)$_2$(NO$_3$)$_3$], Ln = Eu, La, except for Eu2 (see text).The complex synthesized with ligand **9** analyzes as [Eu(L)$_3$(NO$_3$)$_3$].*

2.2 Experimental

2.2.1 General

Phenanthroline was supplied by Merck, triethylamine was supplied by Acros and all other chemicals were purchased from Sigma–Aldrich and used as received.
NMR spectra were recorded on a Bruker DPX-300 spectrometer. Infrared spectra were recorded on a Perkin–Elmer Paragon 1000 FTIR spectrometer equipped with a Golden Gate ATR. Elemental analysis for C, H, N was performed on a Perkin–Elmer 2400 series II analyzer. Excitation and emission spectra were recorded on a Shimadzu RF–5301PC spectrofluoriphotometer equipped with a solid state sample holder and a UV-blocking filter. Photoluminescence quantum yields were determined using an Edinburgh Instruments FLS920 spectrofotometer equipped with an integrating sphere, following a modified version of the procedure reported by de Mello *et al*.[7]. All spectra were corrected for the response of the detection system and reflectivity of the integrating sphere. For lifetime measurements, a pulsed laser source at 355 nm was used as an excitation source on the same machine.
The nitrate salt of Eu(III) was obtained by dissolving Eu_2O_3 in hot concentrated nitric acid to give a clear solution. Subsequent evaporation of the solvent under reduced pressure gave the nitrate salt as a white crystalline compound, for which the composition $Eu(NO_3)_3 \cdot 5H_2O$ was assumed.

2.2.2 X-ray crystal structure determination

For the determination of the structures of **Eu6**, **Eu7** and **Eu9** a crystal was selected for the X-ray measurements and mounted to the glass fiber using the oil drop method. Data were collected at 173 K on a Nonius Kappa CCD diffractometer (Mo-Kα radiation, graphite monochromator, λ = 0.71073 Å) [8, 9]. The intensity data were corrected for Lorentz and polarization effects, and for absorption. The programs COLLECT, SHELXS–97 and SHELXL–97 were used for data reduction, structure solution and structure refinement, respectively [10, 11]. The non-hydrogen atoms were refined anisotropically. The H atoms were introduced in calculated positions and refined with fixed geometry with respect to their carrier atoms. In compound **Eu6** the solvent ethanol is disordered in two positions with population parameters 0.5.
For **Eu8** and **La8**, all reflection intensities were measured at 110(2) K using a KM4/Xcalibur (detector: Sapphire3) with enhanced graphite-monochromated Mo-Kα radiation (λ = 0.71073 Å) under the program CrysAlisPro (Version 1.171.35.11 for **Eu8**, Version 1.171.36.20 for **La8**, Oxford Diffraction Ltd., 2011). The program CrysAlisPro was used to refine the cell dimensions and for data reduction. The structure was solved with the program SHELXS–97 and was refined on F^2 with SHELXL–97 [10]. Analytical numeric absorption corrections based on a multifaceted crystal model were applied using

CrysAlisPro. The temperature of the data collection was controlled using the system Cryojet (manufactured by Oxford Instruments). The H atoms were placed at calculated positions using the instruction AFIX 43 or AFIX 93 with isotropic displacement parameters having values 1.2 times *U*eq of the attached C or N atoms.

2.2.3 Synthesis

*1,10-Phenanthroline-2-carbonitrile, CNphen (**1**)*

The compound was prepared following the procedures reported by Engbersen *et al*. and Corey *et al*. [12, 13]. ^{1}H NMR (300 MHz, MeOD) δ /ppm: 9.25 (dd, 1H), 9.06 (dd, 1H), 8.81 (d, 1H) 8.32-8.20 (m, 4H). IR (ν/cm^{-1}): 3068(br, m), 2230(m), 1584(m), 1506(s), 1486(s), 1417(m), 1403(m), 1390(s), 1296(m), 1313(m), 1135(m), 1098(s), 986(m), 961(w), 950(w), 899(m), 850(vs), 827(s), 816(m), 777(s), 737(vs), 717(s), 652(vs), 628(s), 578(m), 523(m), 461(m), 417(m).

*1,10-Phenanthroline-2-carboxylic acid, HO$_2$Cphen (**2**)*

Following the procedures described by Ten Brink *et al.*, **1** was hydrolyzed to the carboxylic acid [14]. ^{1}H NMR (300 MHz, $CDCl_3$) δ/ppm: 9.16 (d, 1H), 8.65 (d, 1H), 8.60 (dd, 1H), 8.49 (d, 1H), 8.12–8.04 (m, 2H), 7.91 (dd, 1H). IR (ν/cm^{-1}): 3468(m br), 3140(m br), 1700(vs), 1694(vs), 1652(s), 1616(m), 1564(m), 1456(s), 1424(s), 1358(vs br), 1294(s), 1204(s br), 1155(s), 861(vs), 834(s), 792(s), 770(s), 720(vs), 602(s), 536(s br), 419(s), 354(m), 338(m), 324(m).

*Methyl-1,10-phenanthroline-2-carboxylate, MeO$_2$Cphen (**3**)*

According to a procedure reported by Weijnen *et al*., **1** was converted to the methyl carboxylate [15]. ^{1}H NMR (300 MHz, MeOD) δ/ppm: 9.27 (dd, 1H), 8.44 (m, 2H), 8.29 (dd, 1H), 7.89 (m, 2H), 7.70 (dd, 1H), 4.12 (s, 3H). IR (ν/cm^{-1}): 3528(m br), 3410(m br), 1714(vs), 1668(s), 1651(s), 1616(s), 1558(s), 1506(s), 1496(s), 1398(s), 1364(m), 1304(s), 1282(vs br), 1172(s), 1141(s), 1087(s), 1019(s), 971(m), 861(vs), 832(s), 812(m), 772(m), 725(vs), 714(s), 668(s), 628(s), 419(s), 384(s), 374(s), 358(s).

*Ethyl-1,10-phenanthroline-2-carboxylate, EtO$_2$Cphen (**4**)*

A procedure similar to that described for **3** was adopted, except that 25 mL of ethanol was used instead of methanol. ^{1}H NMR (300 MHz, MeOD) δ/ppm: 9.12 (dd, 1H), 8.57 (d, 1H), 8.48 (dd, 1H), 8.39 (d, 1H), 8.00 (m, 2H) 7.81 (dd, 1H) 4.55 (q, 2H), 1.51 (t, 3H).
IR (ν/cm^{-1}): 3488(m br), 3182(m br), 1723(vs), 1684(m), 1616(s), 1507(m), 1456(m), 1442(s), 1404(s), 1302(s), 1278(vs br), 1196(m), 1157(s), 1141(vs), 1088(m), 970(s), 892(w), 861(s), 836(m), 828(m), 814(s), 762(s), 724(vs), 718(vs), 630(s), 492(m vbr), 448(vs), 344(s).

*2-Chloro-1,10-phenanthroline, Clphen (**5**)*

2-Chloro-1,10-phenanthroline was prepared from 1,10-phenanthroline N-oxide obtained from 1,10-phenanthroline as described for **9**, following literature procedures [12, 13]. The N-oxide was converted to 1-methyl-1,10-phenanthrolin-2(1*H*)-one following the procedure given by Kolling [16]. Subsequently, this compound was chlorinated following the procedure given by Halcrow *et al*. [17]. ^{1}H NMR (300 MHz, $CDCl_3$) δ/ppm: 9.06 (dd, 1H), 8.50 (dd, 1H), 8.45 (d, 1H), 7.98 (m, 2H), 7.82–7.75 (m, 2H). IR (ν/cm^{-1}): 3054 (w br), 1621(w), 1582(s), 1553(s), 1494(s), 1440(s), 1414(s), 1387(s), 1312(m), 1212(m), 1152(m), 1140(s), 1123(vs), 1071(s), 870(s), 839(vs), 824(s), 767(s), 730(vs), 711(s), 624(s), 611(s), 574(m), 514(m), 492(m), 420(s), 352(s), 321(m), 314(m).

*2-Methoxy-1,10-phenanthroline, MeOphen (**6**)*

This compound was synthesized from 5 following a procedure reported by Claus et al. [18]. ^{1}H NMR (300 MHz, MeOD) δ/ppm: 9.04 (dd, 1H), 8.44 (dd, 1H), 8.25 (d, 1H), 7.79 (m, 3H), 7.16 (d, 1H), 4.26 (s, 3H). IR (ν/cm^{-1}): 3372(m vbr), 3010(w), 2949(w), 1662(w), 1652(w), 1646(w), 1609(s), 1593(s), 1564(s), 1558(m), 1540(w), 1506(vs), 1464(vs), 1430(m), 1410(s), 1394(m), 1354(vs), 1303(m), 1266(vs), 1225(s), 1132(s), 1075(m), 1020(vs), 914(m), 876(m), 845(vs), 831(vs), 792(m), 770(s), 748(m), 732(s), 718(s), 683(vs), 655(s), 627(s), 569(m), 458(m), 437(s), 396(m), 375(m), 334(m), 316(m).

*2-Ethoxy-1,10-phenanthroline, EtOPhen (**7**)*

A procedure similar to that described for **6** was adopted, using ethanol instead of methanol. ^{1}H NMR (300 MHz, MeOD) δ/ppm: 9.01 (dd, 1H), 8.41 (dd, 1H), 8.22 (d, 1H), 7.75 (m, 3H), 7.12 (d, 1H), 4.76 (q, 2H), 1.48 (t, 3H). IR (ν/cm^{-1}): 3290(m vbr), 2978(m), 1684(m), 1652(m), 1622(s), 1612(s), 1594(s), 1560(s), 1506(s), 1499(s), 1457(vs), 1422(s), 1398(m), 1386(m), 1366(s), 1345(s), 1299(m), 1280(vs), 1226(m), 1139(s), 1098(m), 1076(m), 1043(s), 948(m), 882(m), 848(vs), 832(m), 804(m), 783(s), 740(vs), 718(s), 698(vs), 668(s), 660(s), 626(vs), 583(s), 564(s), 487(s), 429(m), 326(m), 322(m), 314(m).

*2-Amino-1,10-phenanthroline, NH_2Phen (**8**)*

Following the procedure reported by Engel, starting from **5** [19]. ^{1}H NMR (300 MHz, MeOD) δ/ppm: 8.99 (dd, 1H), 8.35 (dd, 1H), 8.06 (d, 1H), 8.74 (d, 1H) 7.65 (dd, 1H), 7.60 (d, 1H), 7.00 (d, 1H). IR (ν/cm^{-1}): 3320(m vbr), 1704(w), 1662(m), 1652(s), 1646(m), 1634(m), 1568(s), 1558(s), 1520(m), 1436(s), 1414(s), 1332(s), 1249(s), 1206(m), 1134(m), 1068(s), 840(s), 813(s), 709(vs), 680(s), 576(s), 552(vs), 403(s), 367(s), 364(s).

*1-Methyl-1,10-phenanthrolin-2(1H)-one, NMeOphen (**9**)*

Phenanthroline was oxidized to its N-oxide using dihydrogen peroxide following the methods reported by Engbersen and Corey [12, 13]. Subsequently, the N-oxide was converted to 1-methyl-1,10-phenanthrolin-2(1*H*)-one using dimethyl sulfate, following the procedure reported by Kolling [16]. ^{1}H NMR (300 MHz, $CDCl_3$) δ/ppm: 8.94 (dd, 1H),

8.18 (dd, 1H), 7.79 (d, 1H), 7.56 (m, 2H), 7.50 (dd, 1H), 6,91 (d, 1H), 4.49 (s, 3H). IR (ν/cm^{-1}): 1657(vs), 1646(vs), 1602(vs), 1539(s), 1505(s), 1468(s), 1418(m), 1271(m), 1196(m), 1166(w), 1128(s), 1035(m), 989(m), 911(m), 843(vs), 783(s), 732(s), 705(s), 656(s), 604(s), 577(m), 546(m), 463(vs).

$[Eu(CNphen)_2(NO_3)_3]\cdot 4H_2O$ ***(Eu1)***

A solution of 0.500 g (2.4 mmol) of **1** in 30 mL ethanol and a solution of 0.348 g (0.8 mmol) $Eu(NO_3)_3\cdot 5H_2O$ in 20 mL ethanol were heated to boiling for 15 minutes to ensure complete dissolution. The $Eu(NO_3)_3$ solution was added to the former slowly. Precipitate formed on cooling to room temperature. The solids was collected on a sintered glass funnel and dried in air to give 0.55 g of powder. Yield 84% based on Eu. IR (ν/cm^{-1}): 3351(m vbr), 3066(m br), 2240(m), 1635(m), 1616(s), 1594(s), 1538(m), 1506(m), 1472(m), 1432(s), 1393(vs), 1299(vs br), 1264(vs), 1232(s), 1214(s), 1152(m), 1040(m), 871(vs), 840(m), 818(m), 788(m), 760(m), 742(m), 730(s), 624(vs), 642(vs), 586(m), 462(vs), 418(s), 385(s), 328(s). Elemental analysis calcd (%) for $C_{26}H_{22}EuN_9O_{13}$ ($Eu(CNphen)_2(NO_3)_3\cdot 4H_2O$): C 38.06, H 2.70, N 15.36; found: C 38.07, H 2.37, N 15.13.

$[Eu(O_2Cphen)_3]\cdot H_2O$ ***(Eu2)***

To a solution of 37 mg (0.18 mmol) of **2** in 10 mL ethanol, 20 mg NEt_3 and 2 mL triethyl orthoformate (TEOF) were added. To a solution of 24 mg (0.06 mmol) $Eu(NO_3)_3\cdot 5H_2O$ in 10 mL ethanol, 4 mL TEOF was added. Both solutions were heated to 70 °C, after which the europium solution was added to the phenanthroline solution. A white precipitate appeared and heating was continued for 30 minutes. The solids were filtered over a paper filter, washed with 30 mL ether and dried in air. Yield 34 mg of microcrystalline powder, 61% based on Eu. IR (ν/cm^{-1}): 3420(m, vbr), 1658(m), 1652(s), 1622(vs), 1616(vs), 1568(vs), 1558(s), 1540(m), 1515(m), 1495(s), 1456(m), 1394(m), 1362(vs br), 1327(s), 1301(s), 1197(m), 1178(m), 1135(m), 1092(m), 1048(m), 910(m), 876(m), 839(m), 818(vs), 743(m), 721(vs), 641(s), 609(s), 421(s), 422(vs), 344(s). Elemental analysis calcd (%) for $C_{39}H_{23}EuN_6O_7$ + 0.1$Eu(NO_3)_3$ (Eu ($O_2Cphen)_3(H_2O)$ + 0.1$Eu(NO_3)_3$): C 53.61, H 2.69, N 10.10; found: C 53.76, H 2.81, N 10.05.

$[Eu(MeO_2Cphen)_2(NO_3)_3]$ ***(Eu3)***

A solution of 0.25 g (1 mmol) of **3** in 20 mL methanol and a solution of 0.15 g (0.33 mmol) $Eu(NO_3)_3\cdot 5H_2O$ in 20 mL methanol were heated to boiling. The $Eu(NO_3)_3$ solution was added to the ligand solution. After the mixture had cooled to room temperature, 20 mL ether was added to aid in precipitation of the complex. The white precipitate was collected by filtration and dried. Yield 64% based on Eu. IR (ν/cm^{-1}): 3400(m, br) 1674(m), 1622(m), 1575(m), 1464(vs, br), 1410(s), 1378(m), 1281(vs, br), 1187(m), 1143(m), 1096(m), 1028(m), 868(m), 840(s), 816(m), 738(m), 721(vs), 668(m), 642(s), 611(m), 472(m), 423(m), 398(m), 376(m), 352(m). Elemental analysis calcd (%) for $C_{28}H_{20}EuN_7O_{13}$

+ 0.14$Eu(NO_3)_3$ ($Eu(MeO_2Cphen)_2(NO_3)_3$ + 0.14$Eu(NO_3)_3$): C 39.02, H 2.34, N 12.06; found: C 39.03 H 2.50 N 11.60.

*[$Eu(EtO_2Cphen)_2(NO_3)_3$] (**Eu4**)*

A solution of 0.070 g (0.28 mmol) **4** in 5 mL ethanol and a solution of 0.059 g (0.14 mmol) $Eu(NO_3)_3 \cdot 5H_2O$ in 5 mL ethanol were heated to boiling. The former solution was slowly added to the latter. Upon cooling a very small amount of a yellowish precipitate formed, which was removed by filtration. Addition of diethyl ether to the filtrate caused a white powder to precipitate from the solution. This precipitate was collected on a Buchner funnel and air dried giving 0.107 g of powder. Yield 89% based on Eu. IR (ν/cm^{-1}): 3300(w br), 1684(m), 1616(m), 1569(m), 1558(w), 1516(m), 1496(s), 1464(s), 1456(s), 1436(s), 1404(s), 1286(vs br), 1096(m), 1029(m), 871(m), 826(s), 739(s), 721(vs), 668(s), 643(s), 610(s), 423(m), 398(m), 350(s), 328(m). Elemental analysis calcd (%) for $C_{30}H_{24}EuN_7O_{13}$ + 0.15$Eu(NO_3)_3$ ($Eu(EtO_2Cphen)_2(NO_3)_3$ + 0.15$Eu(NO_3)_3$): C 40.34, H 2.71, N 11.68; found: C 40.05, H 2.44, N 11.81.

*[$Eu(Clphen)_2(NO_3)_3$] (**Eu5**)*

A solution of 0.13 g (0.6 mmol) of **5** in 3 mL ethanol and a solution of 0.12 g (0.3 mmol) of $Eu(NO_3)_3 \cdot 5H_2O$ in 3 mL ethanol were heated to boiling. The Eu solution was slowly added to the phenanthroline solution. Heating and stirring was continued for 5 minutes. Upon cooling to room temperature, a precipitate formed. The precipitate was collected on a Buchner filter and washed with ethanol. The precipitate was allowed to dry in air. Yield 225 mg, 97% based on Eu. IR (ν/cm^{-1}): 1616(w), 1580(w), 1481(vs), 1424(s), 1374(w), 1294(vs), 1212(m), 1198(m), 1180(w), 1143(m), 1114(w), 1031(m), 995(w), 953(s), 886(s), 809(s), 780(w), 733(vs), 723(s), 638(s), 619(m), 576(w), 556(w), 522(w). Elemental analysis calcd (%) for $C_{24}H_{14}Cl_2EuN_7O_9$ ($Eu(Clphen)_2(NO_3)_3$): C 37.37, H 1.84, N 12.78; found: C 37.56, H 1.76, N 12.66.

*[$Eu(MeOphen)_2(NO_3)_3$] (**Eu6**)*

A solution of 600 mg (2.8 mmol) of **6** in 15 mL ethanol, and a solution of 375 mg (0.88 mmol) $Eu(NO_3)_3 \cdot 5H_2O$ in 10 mL ethanol were heated to boiling for 5 minutes. The salt solution was slowly added to the ligand solution. Precipitate appeared on cooling to room temperature and was collected on a sintered funnel. The precipitate was washed with 4 portions of 30 mL ethanol and dried in air. Yield 0.567 g, 85% based on Eu. IR (ν/cm^{-1}): 1610(m), 1594(m), 1575(m), 1516(s), 1496(s), 1471(vs), 1456(vs), 1436(s), 1418(vs), 1399(m), 1346(s), 1323(vs), 1287(vs), 1240(m), 1181(m), 1156(m), 1122(m), 1092(m), 1052(m), 1035(vs), 903(m), 848(vs), 814(m), 781(m), 740(vs), 728(s), 692(m), 659(m), 642(m), 586(m), 572(m), 490(m), 427(m), 398(m), 374(m), 344(m), 334(m), 327(m), 314(m). Elemental analysis calcd (%) for $C_{26}H_{20}EuN_7O_{11}$ ($Eu(MeOphen)_2(NO_3)_3$): C 41.17, H 2.66, N 12.93; found: C 40.64, H 2.70, N 12.66.

Single crystals were obtained from a diffusion experiment using a Y-tube. One leg of the tube was charged with 300 mg (1.4 mmol) of **6**, while the other was charged with 187 mg (0.44 mmol) of $Eu(NO_3)_3 \cdot 5H_2O$. The tube was filled with ethanol such that the solvent level was 4 mm above the intersection of both legs. After three weeks at room temperature, orange plate-like crystals had formed in the tube.

$[Eu(EtOphen)_2(NO_3)_3]$ ***(Eu7)***

A solution of 640 mg (2.85 mmol) of **7** in 15 mL ethanol and a solution of 407 mg (0.95 mmol) $Eu(NO_3)_3 \cdot 5H_2O$ in 10 mL ethanol were heated to boiling for five minutes. The salt solution was slowly added to the ligand solution. The precipitate that formed on cooling to room temperature was collected on a sintered glass funnel. The precipitate was washed with four portions of 30 mL ethanol and dried in air and in a desiccator. Yield 0.62 g, 64% based on Eu. IR (ν/cm^{-1}): 1612(m), 1593(m), 1575(m), 1512(s), 1472(s), 1456(vs), 1424(m), 1339(s), 1308(vs), 1286(br, vs), 1236(m), 1157(m), 1121(m), 1090(m), 1051(m), 1034(vs), 959(m), 878(m), 845(s), 813(m), 780(m), 739(vs), 727(s), 708(m), 668(m), 655(m), 642(s), 572(m), 510(m), 425(m), 375(m), 358(m), 324(m). Elemental analysis calcd (%) for $C_{28}H_{24}EuN_7O_{11}$ ($Eu(EtOphen)_2(NO_3)_3$): C 42.76, H 3.08, N 12.47; found: C 42.51, H 2.95, N 12.49.

Crystals were obtained as for **Eu6**, except that 25 mg (0.11 mmol) of **7** and 16 mg (0.04 mmol) of $Eu(NO_3)_3 \cdot 5H_2O$ were used. After three weeks at room temperature, yellow plate-like crystals had formed in the tube.

$[Eu(NH_2phen)_2(NO_3)_3]$ ***(Eu8)***

A solution of 0.32 g (1.6 mmol) of **8** in 20 mL ethanol and a solution of 0.23 g (0.54 mmol) $Eu(NO_3)_3 \cdot 5H_2O$ in 10 mL ethanol were heated and stirred at 60 °C for 10 minutes. The salt solution was added drop wise to the ligand solution. A yellow precipitate formed immediately. After cooling to room temperature the precipitate was collected on a sintered funnel and washed with three portions of 20 mL ethanol. The precipitate was allowed to dry in air, yielding 0.33 g (84% based on Eu). IR (ν/cm^{-1}): 3484(m), 3440(m), 3379(m), 3252(m), 1657(m), 1646(s), 1616(m), 1594(m), 1564(m), 1540(w), 1520(m), 1496(vs), 1472(vs), 1456(vs), 1436(s), 1423(s), 1385(vs), 1318(br, s), 1275(s), 1216(m), 1156(m), 1093(m), 1031(s), 841(vs), 811(s), 778(m), 732(s), 721(s), 702(s), 659(s), 643(s), 583(m), 518(m), 448(s), 433(s), 413(vs), 398(vs), 374(s), 349(m), 342(m), 328(s). Elemental analysis calcd (%) for $C_{24}H_{18}EuN_9O_9$ ($Eu(NH_2phen)_2(NO_3)_3$): C 39.57, H 2.49, N 17.31; found: C 39.45, H 2.80, N 16.72. Single crystals of **Eu8** were obtained using the procedure described for **Eu6**, but using 0.15 g (0.75 mmol) of **8** and 0.11 g (0.38 mmol) of $Eu(NO_3)_3 \cdot 5H_2O$ and slow cooling of the reaction mixture to room temperature.

*[La(NH$_2$phen)$_2$(NO$_3$)$_3$] (**La8**)*

The procedure for the synthesis of **Eu8** has been followed, except that 0.21 g (0.5 mmol) La(NO$_3$)$_3$·5H$_2$O was used instead of Eu(NO$_3$)$_3$·5H$_2$O and 0.29 g (1.5 mmol) of **8**. Yield 0.23 g (65% based on La). IR (ν/cm^{-1}): 3482(m), 3431(m), 3379(m), 3246(m), 1645(s), 1588(m), 1562(m), 1465(vs), 1438(vs), 1423(s), 1385(vs), 1317(br, s), 1269(s), 1215(m), 1031(s), 842(vs), 812(s), 775(m), 731(s), 719(s), 701(s), 659(m), 642(s), 582(w), 537(w), 514(w). Elemental analysis calcd (%) for C$_{24}$H$_{18}$LaN$_9$O$_9$ + 0.1La(NO$_3$)$_3$ (La(NH$_2$phen)$_2$(NO$_3$)$_3$ + 0.1La(NO$_3$)$_3$): C 38.55, H 2.43, N 17.42; found: C 38.03, H 2.32, N 17.41. Single crystals were obtained as for **Eu8**.

*[Eu(NMeOphen)$_3$(NO$_3$)$_3$] (**Eu9**)*

0.25 g (1.2 mmol) of **9** was dissolved in 15 mL of ethanol and heated to boiling for 15 minutes until complete dissolution of **9**. To this solution was slowly added a boiling solution of 0.17 g (0.4 mmol) Eu(NO$_3$)$_3$·5H$_2$O in 10 mL ethanol. The mixture was boiled and stirred for 15 more minutes and cooled down to room temperature. The resulting precipitate was collected by filtration, washed with ethanol and allowed to dry in air. Yield 200 mg, 50% based on Eu, of a light yellow powder. IR (ν/cm^{-1}): 1640(s), 1616(w), 1600(m), 1564(s), 1558(s), 1538(vs), 1496(s), 1472(vs), 1456(vs), 1436(m), 1424(s), 1404(s), 1291(br, vs), 1236(s), 1200(m), 1168(m), 1144(m), 1026(s), 989(m), 922(m), 848(vs), 831(m), 816(m), 780(s), 736(s), 708(vs), 668(m), 658(s), 604(s), 578(m), 547(m), 527(m), 478(vs), 398(w), 358(m), 336(w), 326(m), 318(m). Elemental analysis calcd (%) for C$_{39}$H$_{30}$EuN$_9$O$_{12}$ (Eu(NMeOphen)$_3$(NO$_3$)$_3$): C 48.36, H 3.12, N 13.01; found: C 48.88, H 3.18, N 13.26. Crystals suitable for single crystal X–ray diffraction were grown by slow diffusion of an ethanolic solution of 0.10 g (0.48 mmol) of ligand into an ethanolic solution of 0.067 g (0.16 mmol) of Eu(NO$_3$)$_3$·5H$_2$O in a Y-tube over a period of three weeks. Crystals appeared as large orange blocks of sizes up to 0.5 × 0.5 × 2.0 mm^3.

2.3 Results

2.3.1 Synthesis and characterization

All ligands were readily synthesized following procedures reported in literature and were analyzed using IR and NMR spectroscopy. Formation of the corresponding Eu(III) complexes was performed by addition of a hot ethanolic solution of Eu(NO$_3$)$_3$·5H$_2$O to a hot stirred solution of the ligand. The solutions were heated to boiling to ensure complete dissolution of the ligand and inorganic salt and to slow down precipitation of the product. In general, the lanthanoid complexes **Eu1-Eu9** are poorly soluble in ethanol and addition of the lanthanoid nitrate solution to the ligand solution at room temperature leads to the immediate formation of a fine precipitate. Unfortunately, the poor solubility of the compounds severely hampers proper analysis. Attempts were undertaken to analyze the lanthanoid coordination compounds with ESI-MS, but due to the poor solubility and

inherent high kinetic lability of the lanthanoid compounds only signals of the ligands were found in the mass spectra. Elemental analysis was performed to determine the composition of the complexes. All complexes analyze as $[Ln(L)_2(NO_3)_3]$, with the exception of **Eu2**, which analyzes as $[Eu(L)_3]$, and **Eu9**, which analyzes as $[Ln(L)_3(NO_3)_3]$. The deviation between the calculated and found values for the elemental analyses for compounds **Eu2**, **Eu3**, **Eu4** and **La8** are readily explained by the inclusion of minor quantities of $Eu(NO_3)_3$ in the samples, which cannot be removed by recrystallization. The molecular nature of these compounds ensures, however, that these minor impurities do not negatively affect their photoluminescent properties, in contrast to phosphor materials that are based on oxide type compounds. Compounds **Eu6** and **Eu7** were dried prior to elemental analysis and luminescence studies. As a result, the disordered solvent molecule that is observed in the crystal structure (*vide infra*) is not apparent from the elemental analysis. When exposed to air, the initially shiny crystals turn lusterless, indicating that solvent molecules are easily lost. TGA analysis showed that with the exception of **Eu3** and **Eu4**, the compounds are thermally stable to at least 200 °C.

The infrared spectra recorded for the ligands are complicated and show many bands, which makes full assignment of the signals difficult. Signals due to characteristic functional groups can be seen; for example, the signal at 2230 cm^{-1} cm can be attributed to the CN group of **1**, while strong bands around 1700 cm^{-1} recorded for ligands **2-4** is typical for the C=O stretch vibration. The strong band at 1650 cm^{-1} observed for **9** indicates the formation of the carbonyl group. NMR spectra recorded for the ligands agree with the literature, or can be readily assigned to the ligand structures. Comparing the IR spectra obtained for the coordination compounds **Eu1-La8** to those of the ligands reveals strong similarities between them, with minor peak shifts. Additional peaks are observed in the IR spectra of compounds **Eu1** and **Eu3-La8**: all show strong bands around 1030, 1290 and 1490 cm^{-1} that can be ascribed to vibrations of the nitrate ions [20]. Bands around 1650 cm^{-1} are observed for **Eu2-Eu4** due to the C=O stretch, which is slightly lower in energy than observed for the separate ligands, indicating that the carbonyl group is participating in a binding interaction in the complexes.

2.3.2 X-ray crystal structure determination

Projections of the structures of **Eu6-Eu8** are shown in Figure 2.2. Experimental data on the crystal structure determination are given in Table 2.1 for compounds **Eu6-La8** relevant bond lengths and angles are given in Table 2.2. Table 2.3 lists the experimental data, band distances and angles for **Eu9**.

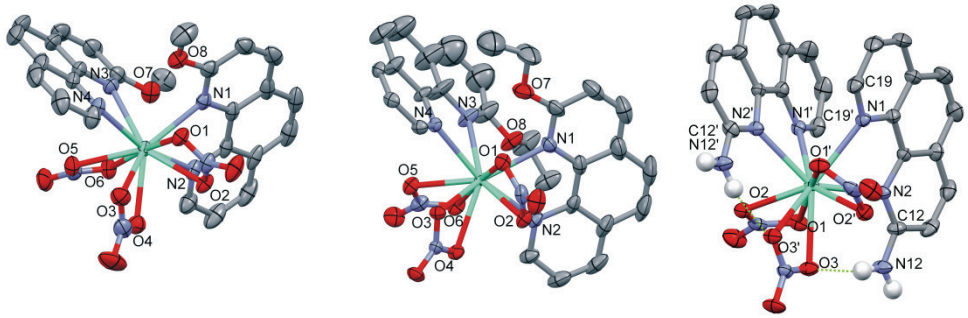

Figure 2.2: From left to right: thermal ellipsoid plots (50% probability contours) of the structures of ***Eu6****, [Eu(MeOphen)$_2$(NO$_3$)$_3$]·EtOH,* ***Eu7****, [Eu(EtOphen)$_2$(NO$_3$)$_3$]·EtOH and* ***Eu8****, [Eu(NH$_2$phen)$_2$(NO$_3$)$_3$] showing the relevant atomic numbering scheme. Only the major disorder component in* ***Eu8*** *and the amine hydrogens and the intramolecular hydrogen bonding interactions are shown; hydrogen atoms and lattice ethanol molecules have been omitted for clarity.*

Table 2.1: Details of the single crystal structure determination of complexes Eu6-La8.

	[Eu6]	**[Eu7]**	**[Eu8]**	**[La8]**
formula	$C_{28}H_{26}EuN_7O_{12}$	$C_{30}H_{30}EuN_7O_{12}$	$C_{24}H_{18}EuN_9O_9$	$C_{24}H_{18}LaN_9O_9$
fw	804.52	832.57	728.43	715.38
crystal size [mm^3]	0.07×0.15×0.20	0.08×0.10×0.10	0.09×0.18×0.37	0.07×0.19×0.23
crystal color	Orange	Yellow	Yellow	Pale yellow
crystal system	Orthorhombic	Triclinic	Monoclinic	Monoclinic
space group	Pbcn (no. 60)	P–1 (no. 2)	C2/c (no. 15)	C2/c (no. 15)
a [Å]	28.145(4)	10.231(1)	10.6715(3)	10.7600(4)
b [Å]	15.023(2)	10.266(1)	18.4251(4)	18.6250(5)
c [Å]	14.735(2)	17.648(1)	13.1230(2)	13.1289(4)
α [°]	90	105.03(5)	90	90
β [°]	90	97.04(5)	93.279(2)	92.011(3)
γ [°]	90	100.07(6)	90	90
V [Å^3]	6230.3(15)	1734.9(7)	2576.1(1)	2629.5(1)
Z	8	2	4	4
d_{calc} [g/cm^3]	1.715	1.594	1.878	1.807
μ [mm^{-1}]	2.089	1.878	2.509	1.697
refl. measured / unique	84459 / 7155	28296 / 7772	8625 / 2958	16280 / 2701
parameters	464	454	206	206
R1/wR2 [I>2σ(I)]	0.0314 / 0.0606	0.0556 / 0.1395	0.0196 / 0.0485	0.0224 / 0.0561
R1/wR2 [all refl.]	0.0531 / 0.0674	0.0657 / 0.1450	0.0221 / 0.0492	0.0253 / 0.0571
S	1.10	1.19	1.03	1.10
$\rho_{min/max}$ [e/Å^3]	–0. 60 / 0.60	–1.45 / 2.13	–0.68 / 0.91	–0.41 / 0.83

Table 2.2: Selected bond distances (Å) and angles (°) for complexes Eu6 - La8.

	[Eu6]	[Eu7]	[Eu8]	[La8]
Bond distance (Å)				
Ln-N1	2.574(3)	2.583(7)	2.600(2)	2.701(2)
Ln -N2	2.579(3)	2.583(6)	2.534(2)	2.622(2)
Ln -N3	2.572(3)	2.572(7)		
Ln -N4	2.590(3)	2.575(6)		
Ln -O1	2.555(2)	2.537(5)	2.528(2)	2.612(2)
Ln -O2	2.514(2)	2.547(5)	2.484(2)	2.585(2)
Ln -O3	2.502(3)	2.518(6)	2.577(2)	2.653(2)
Ln -O4	2.515(3)	2.548(6)		
Ln -O5	2.515(3)	2.545(6)		
Ln -O6	2.544(3)	2.514(5)		
Ln -O7	3.351(3)	3.375(6)		
Ln -O8	3.372(3)	3.411(5)		
Bond angle (°)				
N11-*Ln*-N110	63.65(9)	64.1(2)	64.92(6)	62.75(6)
N21-*Ln*-N210	63.48(9)	63.9(2)		
O31-*Ln*-O32	50.29(7)	50.2(2)	51.00(5)	49.23(6)
O41-*Ln*-O42	51.08(8)	50.5(2)	49.33(5)	48.17(5)
O51-*Ln*-O52	50.45(8)	50.5(2)		

Complexes **Eu6**-**La8** have a ten-fold coordination geometry around the central lanthanoid ion, as a result of two phenanthroline ligands binding in a bidentate mode and three bidentate nitrate ligands. The resulting coordination geometry around the Eu(III) ion is best described as a distorted sphenocorona. Compounds **Eu8** and **La8** are isostructural, with a C_2 axis passing through a nitrato N-O bond and the lanthanoid ion, whereas in **Eu6** and **Eu7** a pseudo C_2 axis is present. The coordination geometry of **Eu6** with the pseudo C_2 axis is shown in Figure 2.3.

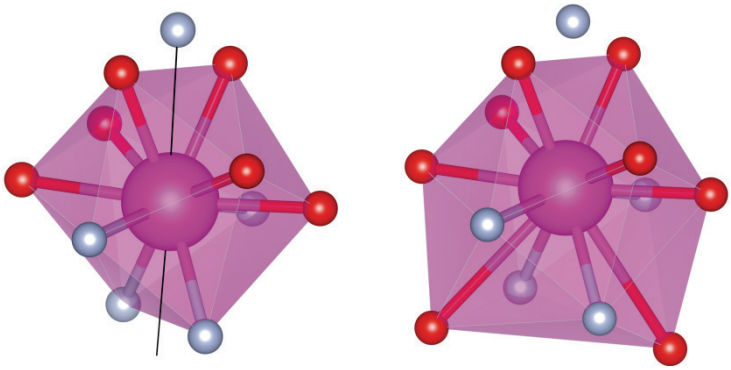

*Figure 2.3: Left: the sphenocorona geometry of **Eu6** with the pseudo C2-axis indicated as a black line passing through the nitrogen of the topmost nitrato ligand and the central Eu(III) ion. The lower two faces are approximately square. Right: expansion of the sphenocorona coordination sphere by inclusion of the second coordination sphere in **Eu6** and **Eu7**, showing additional interactions between the ether oxygen atoms and Eu(III) via the square faces.*

In both **Eu6** and **Eu7**, for each complex a disordered molecule of ethanol is present in the crystal lattice. In **Eu6** and **Eu7**, the Eu-O bond lengths range from 2.502(3) to 2.555(3) Å, while Eu-N bond lengths vary from 2.572(3) to 2.590(3) Å, which is in line with closely related compounds [1, 21]. The coordination angle of the nitrato ligands is around 50° whereas the phenanthroline N-Eu-N angles are around 63°.
The structures of **Eu8** and **La8** are mostly ordered, but the substituted carbon atom with the attached amine group of the phenanthroline ligands is located partially on C12 and partially on C19; the major component of the disordered C–NH_2 group is positioned on C12 (66.3% for **Eu8** and 60.1% for **La8**). In both positions the amine hydrogens form strong intramolecular H-bonding interactions with a coordinated nitrate oxygen atom, having an H···O distance of 1.96 Å in **Eu8** and 2.06 Å in **La8**. Intermolecular H-bonding interactions of the amine hydrogens with nitrate ions influence the packing of the molecules. The coordination bond lengths vary from 2.484(2) Å to 2.577(2) Å for Eu-O and from 2.534(2) Å to 2.600(2) Å for Eu-N. These values are in line with those found for **Eu6** and **Eu7**. In **La8**, the La-O bond distances range from 2.622(2) Å to 2.701(2) Å and from 2.585(2) Å to 2.653(2) Å for La-N. These values are slightly higher than those found for **Eu8** which is readily explained by lanthanoid contraction [21]. A projection of the crystal structure of **Eu9** is shown in Figure 2.4. The structure contains a single Eu(III) ion in the asymmetric unit, and has two molecules in the unit cell. The first coordination sphere of the complex contains three ligands bonded to Eu(III) through the carbonyl oxygen of **9** and three bidentate nitrate ions, resulting in a coordination number of nine around the central ion. Interestingly, all phenanthroline ligands are lying in approximately parallel planes. The geometry around the Eu(III) ion is best described as a highly distorted monocapped square antiprism with the top vertex and a corner of one of the squares being defined by nitrato oxygens, while the other three corners of this square are occupied by the carbonyl oxygens of the ligand. The other square face comprises four nitrato oxygen atoms. The Eu-O bond (Table 2.3) range from 2.322(1) to 2.360(2) Å for the Eu-carbonyl oxygens of the ligands, which can be considered as normal [21]. For the chelating nitrates, Eu-O bond lengths vary from 2.472(2) to 2.550(2) Å. The length of the C=O double bond varies from 1.258(3) to 1.268(4) Å, indicating a slight elongation as compared to C(sp^2)=O bonds that are around 1.20 Å on average [22]. The Eu-O-C bond angles vary markedly within the complex, as can be seen from Table 2.3. π-Stacking interactions play an important role in the crystal structure: the plane-to-plane distances between neighboring phenanthroline rings range from 3.227(1) to 4.097(1) Å. A number of these stacking interactions is shown in Figure 2.4; the distances between the centroids in this particular stacking interaction are 3.77 – 4.41 Å.

Table 2.3: Details of the single crystal structure determination, bond distances (Å) and angles (°) for Eu9.

Details of the experiment		**Bond distances and angles**			
formula	$C_{39}H_{30}EuN_9O_{12}$	*Bond distance* (Å)		*Bond Angle* (°)	
fw	968.68				
crystal size [mm^3]	0.20×0.20×0.10	Eu - O1	2.472(2)	O1 -Eu -O2	51.01(7)
crystal color	Orange	Eu - O2	2.516(2)	O3 -Eu -O4	51.17(6)
crystal system	Triclinic	Eu - O3	2.522(2)	O5 -Eu -O6	50.68(6)
space group	P–1 (no. 2)	Eu - O4	2.486(2)		
a [Å]	10.296(1)	Eu - O5	2.477(2)	C - O7 - Eu	143.8(2)
b [Å]	12.478(1)	Eu - O6	2.550(2)	C - O8 - Eu	152.0(2)
c [Å]	15.661(2)	Eu - O7	2.360(1)	C - O9 - Eu	134.4(2)
α [°]	77.45(1)	Eu - O8	2.322(1)		
β [°]	85.95(1)	Eu - O9	2.350(2)		
γ [°]	69.52(1)				
V [$Å^3$]	1839.8(4)	C - O7	1.265(3)		
Z	2	C - O8	1.258(3)		
d_{calc} [g/cm^3]	1.749	C - O9	1.286(4)		
μ [mm^{-1}]	1.786				
refl. measured / unique	29148 / 8357				
parameters	553				
R1/wR2 [I>2σ(I)]	0.0264 / 0.520				
R1/wR2 [all refl.]	0.0374 / 0.0555				
S	1.09				
$\rho_{min/max}$ [$e/Å^3$]	–0.50 / 0.69				

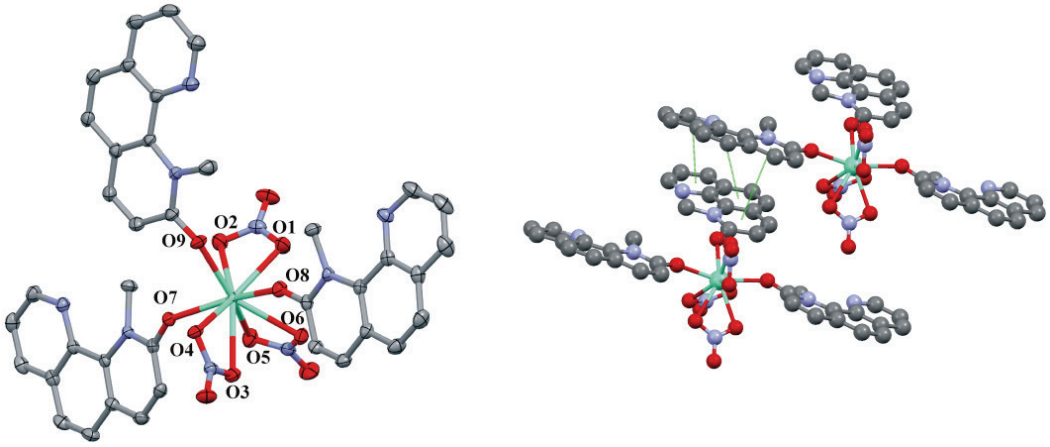

*Figure 2.4: Left: projection of the crystal structure of **Eu9** as thermal ellipsoid plot (50% probability) with the atom numbering scheme indicated. Hydrogen atoms have been omitted for clarity. Right: a projection of part of the structure of **Eu9**, showing the π-stacking interactions.*

2.3.3 Luminescence

The solid state photoluminescence spectra of complexes **Eu1-Eu9** and **La8** are shown in Figure 2.5. Excitation spectra were obtained by constantly monitoring the $^5D_0 \rightarrow {}^7F_2$ transition at 615 nm while scanning the excitation wavelength from 220 to 400 nm. All complexes feature a broad excitation band in the nUV region, originating from phenanthroline-centered excitation. The small spike on the shoulder of the broad band at 395 nm in the spectra of **Eu2**, **Eu5** and **Eu9** can be attributed to direct excitation of the Eu(III) ion *via* the ($^5L_6$, $^5G_2$, $^5L_7$, $^5G_3$) $\leftarrow {}^7F_0$ transition [23]. The excitation maxima for **Eu1**-**Eu8** are all fairly close, and range from 351 to 372 nm. For **Eu9**, the excitation maximum is at 275 nm. The absorption spectra recorded for **Eu1**-**Eu9** and **La8**, shown in Figure 2.6, indeed show broad and strong absorption bands in the near UV region. The emission spectra of **Eu1-Eu7** and **Eu9**, obtained by exciting the compounds in the ligand-centered excitation band, are characteristic for Eu(III) with lines at 580, 595, 615, 649 and 685 nm originating from the $^5D_0 \rightarrow {}^7F_J$ (J = 0, 1, 2, 3, 4) transitions. In all cases, the most dominant line corresponds to the $^5D_0 \rightarrow {}^7F_2$ transition. Different splitting patterns of the fundamental $^5D_0 \rightarrow {}^7F_J$ transition lines are the result from crystal field splitting by different coordination environments around the luminescent center. Photoluminescence quantum yields and lifetimes are listed in Table 2.4. The quantum yields range from 10% for **Eu1** to 79% for **Eu5**, and luminescence lifetimes vary from 0.43 for **Eu1** to 1.57 ms for **Eu2**. Equation 1 was used to fit the experimental decay curves using a least-squares fitting procedure with satisfactory results (R^2 > 99.7% in all cases).

$$I(t) = I(0) + A \cdot \exp\left(\frac{-t}{\tau}\right) \qquad (1)$$

Complex **Eu8**, with 2-aminophenanthroline as a ligand, shows no photoluminescence upon excitation in the (near-) UV region, while the analogous La(III) complex **La8** shows broad band luminescence from 400 to 600 nm.

Table 2.4. Photophysical properties of complexes Eu1-Eu9.

	Φ_{tot} (%)	Ω_2 (10^{-20} cm^2)	Ω_4 (10^{-20} cm^2)	τ_{exp} (ms)	τ_{rad} (ms)	Φ_{Ln} (%)	η_{sens} (%)
Eu1	10	8.82	5.25	0.43	2.56	17	61
Eu2	n.d.	n.d.	n.d.	1.57	n.d.	n.d.	n.d.
Eu3	27	9.75	4.53	0.66	2.37	28	98
Eu4	n.d.	n.d.	n.d.	0.57	n.d.	n.d.	n.d.
Eu5	79	11.93	5.98	1.00	1.94	52	~100
Eu6	20	10.29	4.92	1.04	2.20	47	43
Eu7	24	9.65	4.24	1.13	2.40	47	52
Eu9	22	11.66	0.61	0.74	1.47	50	44

Φ_{tot} (%): Overall photoluminescence quantum yield at 355 nm excitation, τ_{exp}: total lifetime of $^5D_0$ state, Ω_J: Intensity parameters, τ_{rad}: radiative lifetime, Φ_{Ln}: intrinsic quantum yield, η_{sens}: sensitizer efficiency.

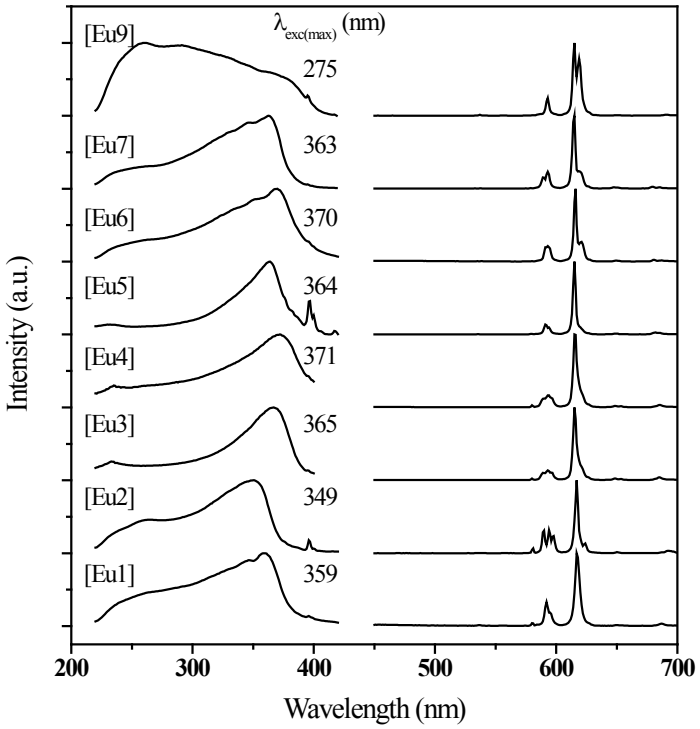

*Figure 2.5: Photoluminescence spectra of **Eu1-Eu9**. The excitation spectra (λ_{em} = 616 nm) are shown on the left hand side with the wavelength of maximum excitation intensity indicated. The right hand side shows the luminescence spectra of the compounds (λ_{exc} = 360 nm), characteristic of Eu(III) with lines at 595, 616, 5, 649 and 685 nm corresponding to $^5D_0 \rightarrow {}^7F_J$, J=1, 2, 3, 4 transitions.*

2.4 Discussion

2.4.1 X-ray crystal structure

The structures as determined for **Eu6**, **Eu7**, **Eu8** and **La8** are rather similar in that the coordination sphere comprises two substituted phenanthrolines binding in a bidentate mode, and three nitrato ligands binding in a bidentate mode. In all cases, the geometry around the *Ln*(III) center closely resembles a distorted sphenocorona. In **Eu6** and **Eu7**, a weak additional interaction between the Eu(III) center and the ether oxygens of the ligand appears to be present, each forming an apex on top of the square faces of the sphenocorona. These are the largest faces of the coordination polyhedron that offer a possibility for bonding to atoms in a second coordination sphere. Figure 2.3 illustrates how these two

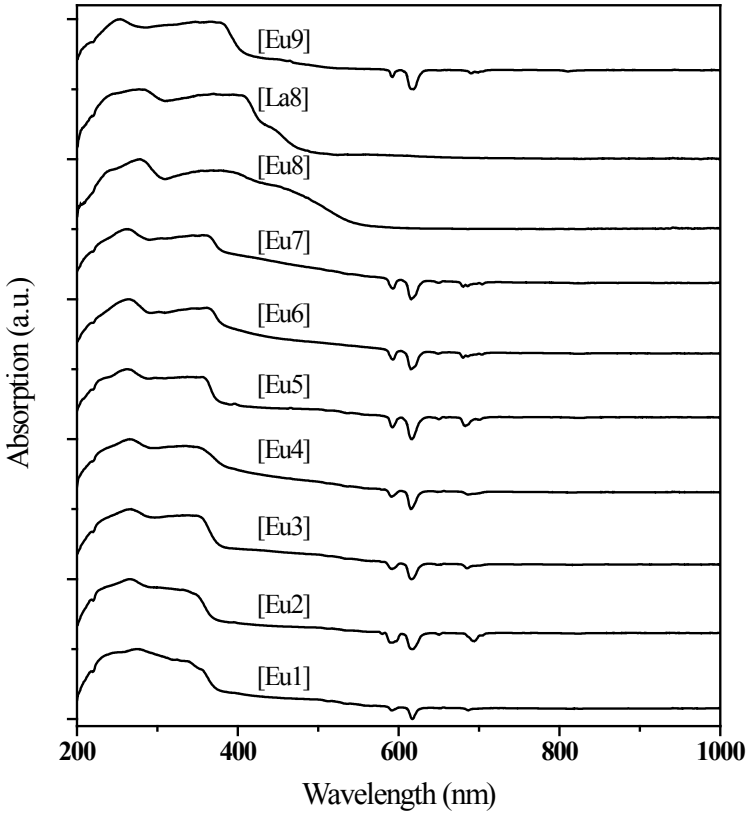

*Figure 2.6: Absorption spectra for compounds **Eu1-Eu9**, showing broad band absorption in the UV and nUV region. The peaks pointing downward are a result of Eu(III) centered emission.*

additional Eu-O bonds are oriented with respect to the polyhedron formed by the first coordination sphere. The bond lengths are 3.351(3) Å for Eu-O7 and 3.372(3) Å for Eu-O8 in **Eu6**. For **Eu7**, the bond lengths of Eu-O7 and Eu-O8 are 3.375(6) Å for Eu-O7 and 3.411(5) Å, respectively. These values are much larger than expected for a normal Eu-O bond, but within the reasonable range for an oxygen atom in the second coordination sphere of Eu(III) [24]. Although complexes **Eu6** and **Eu7** have very similar structures that closely resembles the structure of the Eu(III) complex with unsubstituted phenanthroline, the crystal packing is very different for both compounds [1, 6]. In the structure of **Eu6** and **Eu7**, π-stacking between the phenanthrolines of neighboring complexes with a interplanar distance of 3.400(1) Å and 3.408(6) Å, respectively, is observed, while the distance between two nearest neighbor Eu(III) ions is 9.632(1) Å and 9.440(2) Å, respectively. Compounds **Eu8** and **La8** are isostructural and adopt a structure that closely resembles that of $[Eu(phen)_2(NO_3)_3]$ [1, 6]. The most notable difference, as compared to the complexes **Eu6**, **Eu7** and the parent phenanthroline complex is the non-coplanarity of the *Ln*(III) ion

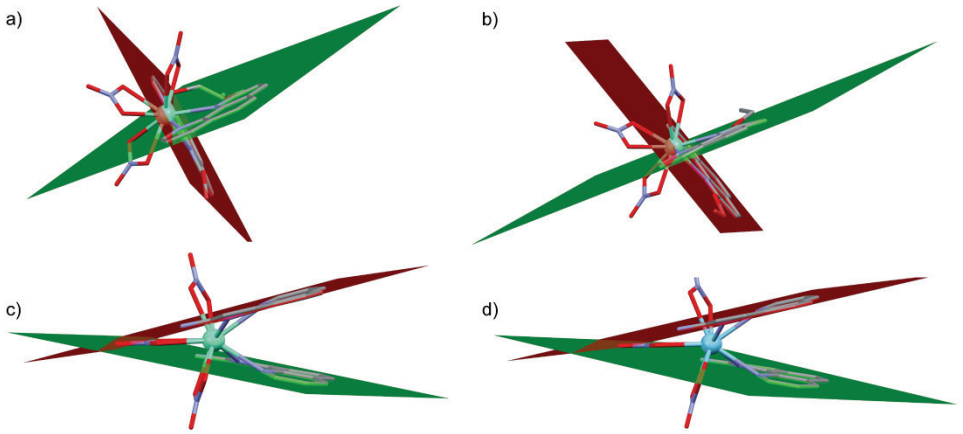

*Figure 2.7: Projections of **Eu6** (a), **Eu7** (b), **Eu8** (c) and **La8** (d) with planes defined by the phenanthroline moieties indicated as red and green surfaces. In **Eu6** and **Eu7**, the Eu(III) ion is in the red plane while in **Eu8** and **La8**, the Ln(III) ion is in neither of the planes.*

with the aromatic system of the phenanthroline ligands. As shown in Figure 2.7, in complexes **Eu8** and **La8**, the planes defined by the ligands do not contain the *Ln*(III) ion. In case of **Eu6** and **Eu7**, the *Ln*(III) ion is in the plane defined by one of the ligands and only slightly out of the plane defined by least-squares fitting to the second ligand. The structure of **Eu9** does not resemble that of **Eu6-La8** because a bidentate mode of coordination *via* the two phenanthroline nitrogens is impossible. Instead, **9** binds through the more available carbonyl oxygen.

2.4.2 Luminescence

Compared to the excitation spectrum of $[Eu(phen)_2(NO_3)_3]$, which has a maximum at 355 nm, the excitation maxima of **Eu1**-**Eu7** are slightly red-shifted, as shown in Figure 2.5. Of the entire series of complexes, **Eu3** and **Eu4** have the highest maximum excitation wavelength at around 370 nm. A slight shift of the maximum to shorter wavelengths is observed only for **Eu2**. At 275 nm, complex **Eu9** has the lowest excitation maximum of the compounds studied. The broad bands are due to the absorption by phenanthroline, indicating clearly that the ligands are acting as antennae. It seems that there is no simple correlation between the electronic properties of the substituent and the optimal excitation wavelength for **Eu1**-**Eu7**. Because in **Eu9** bonding of the ligand through its two nitrogen atoms is not possible, direct comparison of its luminescent properties to those determined for the other Eu(III)-phenanthroline complexes seems inappropriate. The methyl group at one of the nitrogen atoms prevents the bidentate coordination of the phenanthroline molecule, thus hindering the normal mode of coordination to the metal. Instead, the ligand

binds to the lanthanoid ion *via* its ketone moiety. While bèta-diketones have been widely studied as sensitizing ligand for lanthanoid compounds, ketones are generally considered to be poor ligands and thus seem to get less attention. However, complexes of Eu(III) with Michler's ketone, benzophenone and azaxanthones have been studied and are reported to exhibit bright photoluminescence, with quantum yields in solution ranging from 9 to 24% [25-27]. This is in line with the quantum yield determined for **Eu9**, which is 22%.
All compounds except for **Eu8** exhibit luminescence characteristic of Eu(III), with most of the emission intensity arising from the $^5D_0 \rightarrow {}^7F_2$ transition which is of a forced electric dipole (ED) nature. The fact that this transition is much stronger than the $^5D_0 \rightarrow {}^7F_1$ magnetic dipole (MD) transition is in agreement with the structures determined for **Eu6**, **Eu7** and **Eu9**, which show that the Eu ion is situated in a non-centrosymmetric coordination environment [28, 29]. Photoluminescence quantum yields and radiative lifetimes of complexes **Eu1** to **Eu9** are given in Table 2.4. Luminescence lifetimes are in the order of one millisecond, which is as expected for Eu(III) complexes. The most intense luminescence is observed for **Eu5**, which has a high quantum yield of 79%. Complexes **Eu1**, **Eu3**, **Eu5-Eu9** show moderately bright photoluminescence at quantum yields ranging from 10 to 27%; values that are comparable to those found for similar complexes in CH_3CN solution [1]. Complex **Eu8** does not exhibit detectable photoluminescence, which can be due to several reasons. Firstly, a spectral mismatch between the ligand's donor level and the Eu(III) ^5D_J acceptor levels can result in poor energy transfer between the ligand and the metal [30-34]. Since La(III), being a $4f^0$ ion, has no excited states below the ligand's excited states, La(III) complexes can be used to study the ligand-centered energy levels in the presence of a lanthanoid ion [35, 36]. Since no ligand-to-metal energy transfer can take place in these complexes, the ligand-centered triplet states can be determined from the phosphorescence spectrum. The room temperature emission spectrum recorded for **La8** (see supporting information) shows an emission band with a maximum at 488 nm (20,500 cm^{-1}), which is well above the $^5D_0$ resonance level of Eu(III) at 17,300 cm^{-1}, suggesting that energy transfer should be possible [37]. Secondly, the absence of photoluminescence in **Eu8** can be explained by the presence of a quenching mechanism, for example *via* a low-lying ligand to metal charge transfer (LMCT) state. The presence of a low lying LMCT state near the energy of the excited ^5D_J multiplet of Eu(III) is known to compete with the ligand to metal energy transfer, and can result in quenching of luminescence [33, 38]. A low energy LMCT state can be expected for lanthanoid complexes in which the ligands have a low oxidation potential and the lanthanoid ion a high electron affinity, as is the case for Eu(III) [34]. Unlike complex **La8**, which has a pale color, **Eu8** has a deep yellow color, which suggests that an LMCT transition might be present. As can be seen from Figure 2.6, the absorption spectra for compounds **Eu8** and **La8** are indeed different: both show a ligand-centered absorption band that extends to approximately 420 nm, but **Eu8** has an additional absorption that extends to almost 500 nm. As the compounds are the same except for the central ion, this difference can only be explained by the difference in chemical

nature of the lanthanoid ions. Finally, an explanation can be found from the crystal structure. It has been suggested that a rigid planar structure of the ligand within the complex is beneficial for energy transfer [39]. As the Eu(III) ion is not lying in the plane defined by the planar ligand molecule, ligand-to-metal energy transfer can be hampered.

2.4.3 Analysis of the emission spectra

The Judd-Ofelt theory (JO theory) provides a powerful framework for analysis of the intensities of the forced ED transitions in the lanthanoid ions [40, 41]. According to JO theory, the intensity of a forced ED transition depends on only three intensity parameters, Ω_λ, $\lambda = 2, 4, 6$, that contain information on the local structure around the lanthanoid ion, such as the symmetry and the degree of covalency of the bonds [42-45]. Details on the JO theory are outlined in section 1.6 of this thesis. Because for the Eu(III) ion, the transition $^5D_0 \rightarrow {}^7F_1$ has no electric dipole contribution so it can be considered practically insensitive to the surroundings of the Eu(III) ion. The strength of this transition has been derived theoretically ($D_{MD} = 9.6 \cdot 10^{-42}$ esu^{2}cm^2)[46] and can be used as an internal reference [44]. On the other hand, the transitions $^5D_0 \rightarrow {}^7F_{2,\,4,\,6}$, are of a purely forced electric dipole character and are described by JO theory. Using the $^5D_0 \rightarrow {}^7F_1$ as an internal reference and using equations 10 and 11 from Chapter 1, the JO parameters can be calculated from the emission spectrum. Relative intensities of the transitions are readily found from the spectrum by integration, provided that that the spectrum represents the relative photon flow [47]. Thus, equation 2 can be used as a theoretical expression for the intensity of the $^5D_0 \rightarrow {}^7F_{2,4,6}$ transitions. The values for the matrix elements used have been calculated and are listed in Table 1.7 [44, 48].

$$\frac{I_{J,exp}}{I_{1,exp}} \propto \frac{A_{0-J}}{A_{0-1}} = \left(\frac{\upsilon_J}{\upsilon_1}\right)^3 \cdot \frac{n\left(n^2+2\right)^2}{9n^3} \cdot \frac{e^2}{D_{MD}} \cdot \sum_{\lambda=2,4,6} \Omega_\lambda \langle J||U^\lambda||J'\rangle \qquad (2)$$

Here, $I_{J,exp}$ represents the experimentally observed intensity of a $^5D_0 \rightarrow {}^7F_J$ transition, υ_J and υ_1 the wavenumber of the $^5D_0 \rightarrow {}^7F_J$ and $^5D_0 \rightarrow {}^7F_1$ transitions, respectively and n the average refractive index of the medium around the Eu(III) ion. Since the $^5D_0 \rightarrow {}^7F_6$ transition was not detected, Ω_6 could not be determined [49, 50]. The Judd-Ofelt intensity parameters have been calculated for compounds **Eu1**-**Eu7**, and are given in Table 2.4. An average refractive index of 1.5 was used in the calculations [51, 52]. It is known that the intensity ratio $I(^5D_0 \rightarrow {}^7F_2) / I(^5D_0 \rightarrow {}^7F_1)$ of the ED vs. MD transitions is a measure of the site symmetry of Eu(III). The higher this ratio, the further the site symmetry departs from inversion symmetry [28]. From Eq. 2 it is obvious that the magnitude of Ω_2 directly depends on this ratio. In general a large Ω_2 is indicative of a low site symmetry and a covalent character of the chemical bonds to the *Ln*(III) ion [43, 53]. From the emission spectra shown in Figure 2.5, it is clear that the $^5D_0 \rightarrow {}^7F_2$ transition is much more intense than the $^5D_0 \rightarrow {}^7F_1$ transition, resulting in high Ω_2 parameters. There seems to be no well-

defined interpretation of the Ω_4 parameter [43]. From Chapter 1, Eq. 10 and 11, it is possible to estimate the radiative lifetime of the complexes. From Eq. 10 in Chapter 1, $A_{0\text{-}1}$ can be calculated (~49 s^{-1}), while the Einstein coefficients for the other transitions can be found from their intensities relative to that of the $^5D_0 \rightarrow {}^7F_1$ transition. The total emissive relaxation rate of the $^5D_0$ state, A_T, is found using equation 12 in Chapter 1. The radiative lifetime τ_{rad} of the emissive state is simply the reciprocal of A_T and is given in Table 2.4. From the experimentally obtained lifetime, τ_{exp} of the $^5D_0$ state and τ_{rad}, the intrinsic quantum yield Φ_{Ln} of the lanthanide ion can be calculated from τ_{exp} / τ_{rad}. The experimentally determined lifetime contains contributions of radiative and non-radiative decay processes of the emissive state, and Φ_{Ln} indicates the relative contribution of radiative transitions. The intrinsic quantum yields have been calculated and are given in Table 2.4. The values range from 17 to 52%, indicating that non-radiative decay processes contribute substantially to the depopulation of the $^5D_0$ state. From Φ_{Ln} and the overall photoluminescence quantum yield Φ_{tot} the efficiency of the sensitization process η_{sens} can be estimated from the relation $\Phi_{tot} = \eta_{sens} \times \Phi_{Ln}$ [54]. It indicates how effective the ligand is at transferring energy to the luminescent center. The ligands in **Eu3** and **Eu5** seem to be particularly effective at sensitizing Eu(III) luminescence, with the main quenching mechanism being non-radiative deactivation of the luminescent center.

2.5 Conclusion

Eight new europium(III) complexes with different 1,10-phenanthroline ligands substituted on the 2-position have been synthesized in yields ranging from 43% to 89%. One isostructural lanthanum(III) compound has been synthesized for the estimation of the ligand's triplet excited state. In addition, 1-methyl-1,10-phenanthrolin-2(1*H*)-one has been used as a ligand for the first time, using Eu(III) as a central ion. The resulting complex is described by $[Eu(L)_3(NO_3)_3]$ wherein the ligand is bound to Eu(III) in a monodentate fashion *via* its carbonyl oxygen. The other complexes all analyze as $[Eu(L)_2(NO_3)_3]$ except for $[Eu(O_2Cphen)_3]$. Solid state photoluminescence studies on the complexes reveal ligand centered excitation for all complexes except **Eu8**, which suggests that 2-amino-1,10-phenanthroline is unsuitable for sensitizing Eu(III) luminescence. A low lying charge-transfer band provides a means of non-radiative relaxation of the $^5D_0$ level on the Eu(III) ion. The luminescent complexes are efficiently excited in the near UV region and exhibit medium to high photoluminescence quantum yields. Compared to $[Eu(phen)_2(NO_3)_3]$, the excitation maximum of **Eu1**, **Eu3**, **Eu4**, **Eu6** and **Eu7** has shifted to longer wavelengths. There seems to be, however, no clear correlation between the electronic properties of the ligand substituent on the excitation maximum of the complex. Although the crystal structure determinations show similar coordination geometries for the lanthanoid ions, the crystal packings of **Eu6**, **Eu7** and **Eu8** are different. Notably, the Eu(III) ion in **Eu8** is not residing in the plane of the sensitizing ligand, which may be another cause of the ligand-to-metal energy transfer to be severely hampered. This suggests

that not only the electronic properties of the substituents should be considered when analyzing the antenna properties, but also the steric demands. The emission spectra are characteristic for Eu(III) centers in a non-centrosymmetric coordination site, which for **Eu6** and **Eu7** is confirmed by single crystal X-ray diffraction data. Analysis of the spectral intensities shows a significant contribution of non-radiative processes that quench the luminescence of the $^5D_0$ level on Eu(III), resulting in low intrinsic quantum yields. The nUV excitation properties and the highly monochromatic emission of **Eu4** and **Eu6** make these compounds suitable for application in nUV LED-chips, but the relatively low quantum yields limit their application as phosphor materials in PC-WLEDs.

2.6 References

[1] Z. Pan, G. Jia, C.-K. Duan, W.-Y. Wong, W.-T. Wong, and P.A. Tanner, *Eur. J. Inorg. Chem.*, 2011 (2011) 637-646.

[2] M.F. Belian, H.J. Batista, A.G.S. Bezerra, W.E. Silva, G.F. de Sá, and S. Alves Jr, *Chem. Phys.*, 381 (2011) 29-34.

[3] M.O. Ahmed, J.-L. Liao, X. Chen, S.-A. Chen, and J.H. Kaldis, *Acta Crystallogr., Sect. E: Struct. Rep. Online*, 59 (2003) m29-m32.

[4] C. Xu, *J. Rare Earth.*, 28 (2010) 854-857.

[5] B. Yan, H.-j. Zhang, S.-b. Wang, and J.-z. Ni, *Mater. Chem. Phys.*, 51 (1997) 92-96.

[6] A.G. Mirochnik, B.V. Bukvetskii, P.A. Zhikhareva, and V.E. Karasev, *Russ. J. Coord. Chem.*, 27 (2001) 443-448.

[7] J.C. de Mello, H.F. Wittmann, and R.H. Friend, *Adv. Mater.*, 9 (1997) 230-232.

[8] T. Kottke and D. Stalke, *J. Appl. Crystallogr.*, 26 (1993) 615-619.

[9] Nonius, *COLLECT*, *Nonius BV, Delft, The Netherlands*, 2002.

[10] G.M. Sheldrick, *Acta Crystallogr., Sect. A: Found. Crystallogr.*, 64 (2008) 112-122.

[11] G.M. Sheldrick, *SHELXS–97*, *Bruker AXS Inc., Madison, Wisconsin*, 1997.

[12] J.F.J. Engbersen, A. Koudijs, M.H.A. Joosten, and H.C. Vanderplas, *J. Heterocycl. Chem.*, 23 (1986) 989-990.

[13] E.J. Corey, A.L. Borror, and T. Foglia, *J. Org. Chem.*, 30 (1965) 288-290.

[14] G.J. ten Brink, I. Arends, M. Hoogenraad, G. Verspui, and R.A. Sheldon, *Adv. Synth. Catal.*, 345 (2003) 1341-1352.

[15] J.G.J. Weijnen, A. Koudijs, and J.F.J. Engbersen, *J. Chem. Soc., Perkin Trans. 2*, (1991) 1121-1126.

[16] L. Kolling, Phenanthroline-Comprising Complexes, Pat.no US2010/234548 A1k US2010/234548 A1, 2010.

[17] B.E. Halcrow and W.O. Kermack, *J. Chem. Soc.*, (1946) 155-157.

[18] K.G. Claus and J.V. Rund, *Inorg. Chem.*, 8 (1969) 59-63.

[19] Y. Engel, A. Dahan, E. Rozenshine-Kemelmakher, and M. Gozin, *J. Org. Chem.*, 72 (2007) 2318-2328.

[20] V. Tsaryuk, V. Zolin, L. Puntus, V. Savchenko, J. Legendziewicz, J. Sokolnicki, and R. Szostak, *J. Alloys Compd.*, 300–301 (2000) 184-192.

[21] A.G. Orpen, L. Brammer, F.H. Allen, O. Kennard, D.G. Watson, and R. Taylor, *J. Chem. Soc., Dalton Trans.*, (1989) S1-S83.

[22] *CRC Handbook of Chemistry and Physics, 85th edition*, 2005: CRC Press, Boca Raton.
[23] W.T. Carnall, P.R. Fields, and K. Rajnak, *J. Chem. Phys.*, 49 (1968) 4412-4423.
[24] D. Parker, R.S. Dickins, H. Puschmann, C. Crossland, and J.A.K. Howard, *Chem. Rev.*, 102 (2002) 1977-2010.
[25] M.H.V. Werts, M.A. Duin, J.W. Hofstraat, and J.W. Verhoeven, *Chem. Commun.*, (1999) 799-800.
[26] A. Beeby, L.M. Bushby, D. Maffeo, and J.A.G. Williams, *J. Chem. Soc., Perkin Trans. 2*, (2000) 1281-1283.
[27] P. Atkinson, K.S. Findlay, F. Kielar, R. Pal, D. Parker, R.A. Poole, H. Puschmann, S.L. Richardson, P.A. Stenson, A.L. Thompson, and J.H. Yu, *Org. Biomol. Chem.*, 4 (2006) 1707-1722.
[28] R. Reisfeld, E. Zigansky, and M. Gaft, *Mol. Phys.*, 102 (2004) 1319 - 1330.
[29] B. Francis, D.B.A. Raj, and M.L.P. Reddy, *Dalton Trans.*, 39 (2010) 8084-8092.
[30] J.-C.G. Bünzli, S. Comby, A.-S. Chauvin, and C.D.B. Vandevyver, *J. Rare Earth.*, 25 (2007) 257-274.
[31] M. Latva, H. Takalo, V.M. Mukkala, C. Matachescu, J.C. Rodriguez-Ubis, and J. Kankare, *J. Lumin.*, 75 (1997) 149-169.
[32] L. Armelao, S. Quici, F. Barigelletti, G. Accorsi, G. Bottaro, M. Cavazzini, and E. Tondello, *Coord. Chem. Rev.*, 254 (2010) 487-505.
[33] S. Petoud, J.-C.G. Bünzli, T. Glanzman, C. Piguet, Q. Xiang, and R.P. Thummel, *J. Lumin.*, 82 (1999) 69-79.
[34] W.M. Faustino, O.L. Malta, and G.F. de Sa, *J. Chem. Phys.*, 122 (2005) 054109.
[35] L. Prodi, M. Maestri, R. Ziessel, and V. Balzani, *Inorg. Chem.*, 30 (1991) 3798-3802.
[36] N.M. Shavaleev, S.V. Eliseeva, R. Scopelliti, and J.-C.G. Bünzli, *Chem.-Eur. J.*, 15 (2009) 10790-10802.
[37] W.T. Carnall, P.R. Fields, and K. Rajnak, *J. Chem. Phys.*, 49 (1968) 4450-4455.
[38] V. Tsaryuk, K. Zhuravlev, V. Kudryashova, V. Zolin, J. Legendziewicz, I. Pekareva, and P. Gawryszewska, *J. Photochem. Photobiol., A*, 197 (2008) 190-196.
[39] Y.S. Yang, M.L. Gong, Y.Y. Li, H.Y. Lei, and S.L. Wu, *J. Alloys Compd.*, 207–208 (1994) 112-114.
[40] B.R. Judd, *Phys. Rev.*, 127 (1962) 750-761.
[41] G.S. Ofelt, *J. Chem. Phys.*, 37 (1962) 511-520.
[42] J.H.S.K. Monteiro, I.O. Mazali, and F.A. Sigoli, *J. Fluoresc.*, 21 (2011) 2237-2243.
[43] H. Liang, Z. Zheng, Q. Zhang, H. Ming, B. Chen, J. Xu, and H. Zhao, *J. Mater. Res.*, 18 (2003) 1895-1899.
[44] M.H.V. Werts, R.T.F. Jukes, and J.W. Verhoeven, *Phys. Chem. Chem. Phys.*, 4 (2002) 1542-1548.
[45] C. Görller-Walrand and K. Binnemans, *Spectral intensities of f-f transitions*, in *Handbook on the Physics and Chemistry of Rare Earths*, 1998, Elsevier. 99-264.
[46] The dipole strength is expressed here in CGS units. As 1 esu ≈ 3.33564×10^{-10} C, one finds that 9.6×10^{-42} esu^{2}cm^2 equals 1.06814×10^{-64} C^{2}m^2 in SI units.
[47] J.W. Verhoeven, *Pure Appl. Chem.*, 68 (1996) 2223-2286.
[48] L. Huang, L. Cheng, H. Yu, L. Zhou, J. Sun, H. Zhong, X. Li, J. Zhang, Y. Tian, Y. Zheng, T. Yu, J. Wang, and B. Chen, *Physica B*, 406 (2011) 2745-2749.

[49] L. Đačanin, S.R. Lukić, D.M. Petrović, M. Nikolić, and M.D. Dramićanin, *Physica B*, 406 (2011) 2319-2322.
[50] R. Balakrishnaiah, R. Vijaya, P. Babu, C.K. Jayasankar, and M.L.P. Reddy, *J. Non-Cryst. Solids*, 353 (2007) 1397-1401.
[51] C.A. Kodaira, H.F. Brito, O.L. Malta, and O.A. Serra, *J. Lumin.*, 101 (2003) 11-21.
[52] M.E. de Mesquita, S.A. Júnior, F.R.G. e Silva, M.A. Couto dos Santos, R.O. Freire, N.B.C. Júnior, and G.F. de Sá, *J. Alloys Compd.*, 374 (2004) 320-324.
[53] H. Ebendorff-Heidepriem, D. Ehrt, M. Bettinelli, and A. Speghini, *J. Non-Cryst. Solids*, 240 (1998) 66-78.
[54] J.-C.G. Bünzli, *Chem. Rev.*, 110 (2010) 2729-2755.